Numerical modeling of the formation of Indo-Sinian peraluminous granitoids in Hunan Province: Basaltic underplating versus tectonic thickening

WANG Yuejun (王岳军)[1], Y. Zhang[2], FAN Weiming (范蔚茗)[1], XI Xianwu (席先武)[1], GUO Feng (郭 锋)[1] & LIN Ge (林 舸)[1]

1. Guangzhou Institute of Geochemistry, Chinese Academy of Sciences, Guangzhou 510640, China;
2. CSIRO Division of Exploration & Mining, Perth 6109, Australia
Correspondence should be addressed to Wang Yuejun (email: yjwang@ms.csig.ac.cn)

Received March 23, 2002

Abstract The genesis of Indo-Sinian granitic plutons with peraluminous and potassium-rich affinities from Hunan Province, China has been investigated by numerical modeling using the numerical code FLAC. On the basis of the regional geological evolution in South China, we employed a realistic numerical model in an attempt to unravel the influences of basaltic underplating and tectonic crustal thickening on the crustal anatexis. Heat production derived from basaltic underplating (e.g. ca. 220 Ma gabbro xenoliths) can result in dehydration melting of fluid-bearing minerals in crustal rocks such as gneisses and metapelites, but its effect is limited in a relatively short time span (5—15 Ma) and on a small scale. Accordingly, it is very difficult for basaltic underplating to generate the large-scale Indo-Sinian granitic bathliths unless voluminous mafic magmas had been underplated at the lower/middle crust during this period. Alternatively, crustal thickening induced by tectonic compression can also lead to geothermal elevation, during which the temperature at the boundary between lower and middle crusts can be up to or greater than 700℃, triggering dehydration melting of muscovite in gneiss and metapelite. The proportion of melts from muscovite-induced dehydration melting is close to critical melt percentage (≥20%) once the thickening factor reaches 1.3. These melts can be effectively transferred to the crust-level magma chamber and form large-scale granitic batholiths. In combination with the Indo-Sinian convergent tectonic setting in South China as well as sparse outcrops of contemporary mafic igneous rocks, we consider that tectonic crustal thickening is likely to be the predominant factor controlling the formation of the Indo-Sinian peraluminous and potassium-rich granitoids in Hunan Province.

Keywords: Indo-Sinian granitoids, dehydrated melting, basaltic undedrplating, tectonic thickening, numerical modeling, Hunan Province.

The Indo-Sinian granitoids in South China are mainly distributed in Hunan and Jiangxi provinces as well as in the Guangxi Zhuang Autonomous Region (Guangxi in short). In Hunan Province, the Indo-Sinian granitic plutons are confined by the Chenzhou-Linwu fault in the east and the Xupu-Jinxian fault in the west, respectively (fig. 1). Lithologically, they are composed of strongly peraluminous-slightly aluminous (A/CNK>1.05) and potassium-rich granites, adamellites and granodiorites, occurring as batholiths or stocks along deep-fault planes or fault intersections (fig. 1). These granodioritic-granitic intrusions, emplaced at ca. 200—240 Ma, partially at 260

Ma± in Hunan Province[1], are characterized by remarkably negative Eu anomalies (δEu = 0.18 — 0.56) and δ O^{18} value of 9.27‰—17.36‰ as well as higher Rb/Sr ratio (> 1.0). The initial $^{87}Sr/^{86}Sr$ ratio ranges from 0.7136 to 0.7264 and $\varepsilon_{Nd}(t)$ from −11 to −17, similar to the Sr-Nd isotopic compositions of gneisses in South China, which were usually interpreted as the remelting products of middle/upper crustal rocks[2,3].

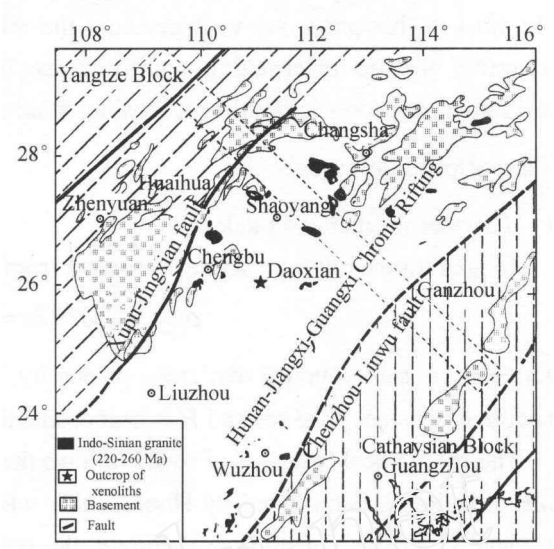

Fig. 1. Simplified geological map of the Indo-Sinian peraluminous and potassium-rich granites in the Hunan-Jiangxi area. The defined area denotes the modeling region.

The Indo-Sinian tectonic evolution and genesis of the contemporary granites in South China have long been debated, and different hypotheses, such as the early Mesozoic Alpine-type collision[4,5] and intracontinental subduction/collision scenarios, have been proposed. The early Mesozoic collision/subduction hypothesis proposed that the Indo-Sinian granites were the products of an island-arc setting. However, more and more evidence strongly argue against the presence of an ocean and the involvement of oceanic- or arc-continental subduction/collision in the interior of the South China block (SCB) during early Mesozoic[6—8]. Alternatively, based on the early Mesozoic deformation and structures, such as the widespread fold-thrusting styles in the region, the intracontinental subduction/collision model suggested that a long-evolving rift should have been existent in the Hunan-Jiangxi-Guangxi area since the Paleozoic[9]. Thus the Indo-Sinian granitoids exposed in this area were possibly the product of tectonic crustal thickening. More and more evidence for mafic magmatism in South China in recent years suggests that multi-episode lithospheric extension and basic magma underplating were developed in the area since the early Mesozoic[10—14]. The emplacement of mafic magmas might provide heat sources to reheat the crust and led to the melting of crustal rocks. Therefore, basaltic underplating undoubtedly represents another possible mechanism for the genesis of these Indo-Sinian granitic plutons. However, the lack of quantitative understanding of thermal-mechanical interactions in all these previous studies on the genesis of the Indo-Sinian granite appears to hamper our understanding of the tectonic evolution of South China.

Based on the information about the regional geological evolution[15—19], we constructed a numerical model using the code FLAC (Fast Lagrangian Analysis of Continua)[1)], in an attempt to unravel the thermal influence of tectonically crustal thickening and basaltic underplating. Our

1) Itasca, Fast Lagrangian Analysis of Continua, User Manual, Vol. 3.2, Minneapolis: Itasca Consulting Group Inc., 1992.

main aims in this paper are to understand the relationship between crustal anatexis and crustal thickening, basaltic underplating, and to discuss the mechanism feasible for the genesis of these Indo-Sinian granitoids under the regional tectonic regime in the Mesozoic.

1 Description of model

1.1 Thermal-mechanical model

Temperature evolution can be calculated from heat conduction equation[20]

$$\rho_{(Z,T)}C_{(T)}\partial T/\partial t = K_{(T)}\nabla^2 T + H,$$

where $K_{(T)}$ is heat conductivity, $\rho_{(Z,T)}$ is density, Z is depth, T is temperature in ℃, $C_{(T)}$ is heat capacity at constant pressure and H is heat production per unit of mass.

The mechanical behavior of rocks follows the elastic-plastic constitutive law. The elastic part of deformation is determined by Hooke's law while the plastic is governed by a non-associated flow law[21]. In this constitutive rheology, the rock is subject to homogeneous elastic deformation[22,23] before a yield stress is reached. Then irrecoverable plastic deformation occurs with continuous load once the maximum yield stress is reached (the Mohr-Coulomb yield criterion). The total strain of the material is the sum of the elastic and plastic components, i.e.

$$\Delta\varepsilon = \Delta\varepsilon^{e} + \Delta\varepsilon^{p},$$

where $\Delta\varepsilon^{e}$ is the elastic strain component and $\Delta\varepsilon^{p}$ is the plastic strain component. The results from the experimental studies of rock deformation suggested that the crustal deformation can be effectively described by the elastic-plastic rheological behavior[24].

1.2 Tectonic-geological model

It is generally believed that the Yangtze and Cathaysian blocks were united by subduction/collision during the Neoproterozoic, constituting part of the Rodinia supercontinent[25]. The breakup of the Rodinia supercontinent resulted in the formation of transtensional basins in the time interval of 820—800 Ma[25,26], where the excessively thick turbidites of secondary deep-sea (or deep-sea) were deposited. The materials in the Cathaysian Block in its east portion were extensively eroded into the oceanic basins (or sea) in Hunan, Jiangxi and Guangxi, where the sedimentary rocks of carbonate platform were developed in the Yangtze Block at its west during the early Paleozoic. The shallow-sea carbonate platform sedimentary rocks occurred in the interior of the Yangtze and Cathaysian blocks, whereas a rifting-type intraplate extensional basin characterized by the abyssal sediments including carbonate, radiolarian-bearing silicalite and detritus strata was developed in the Hunan-Guagxi-Jiangxi area during the late Paleozoic[26,27]. The total thickness of the detrital and carbonate sequences is over 12—15 km in the intraplate extensional basin in the Hunan-Jiangxi-Guangxi area since Sinian while only 3—5 km thickness on its sides, displaying a non-symmetric basin geometry in which the thickness of sediments in its east portion is greater than that in the west portion[2,3,26—28]. During the early Mesozoic, the excessively thick Pa-

leozoic sedimentary rocks were strongly deformed, producing top-to-NW thrusting in the area between the east of the Xuefeng Mountain and the west of the southeastern Hunan Province[2,3,28,29]. Based on the data mentioned above, a geological model was constructed and is shown in fig. 2(a). In the model, the trough corresponds to the area between the Xuefeng Mountain and the southeastern Hunan Province, and the segments of the section to the east and west of the trough represent the Cathaysian Block and Yangtze Block, respectively.

It is generally accepted that the melting behavior of rocks in the crust can be attributed to its mineral assemblage compositions and lithological associations. The geochemical data from late Mesozoic basaltic rocks and their hosting xenoliths as well as geophysical profiles in Hunan

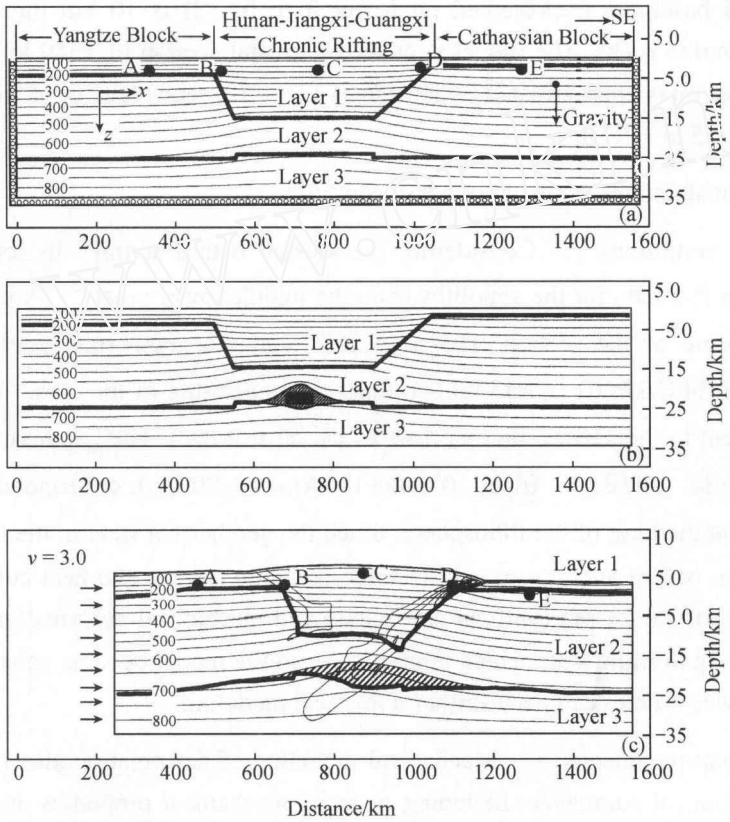

Fig. 2. The outline and results of the thermal-mechanical model for the generation of peraluminous and potassium-rich Indo-Sinian granitoids in the Hunan-Jiangxi-Guangxi area. (a) The initial geometrical feature of the model and temperature distribution (°C). (b) Temperature distribution showing the maximum thermal perturbation due to basaltic underplating into the middle/lower crust. The black box beneath the trough represents the underplating magma (50 km × 1 km) and the shaded area surrounding the box indicates the region with the maximum thermal perturbation. (c) The temperature and shear stress distributions of a model involving a horizontal shortening and a crustal thickening of maximum 43 km. The shaded area denotes the extent of the muscovite dehydration melting and closed lines indicate the locations of the maximum shear stresses (maximum is 2 MPa and the interval is 0.25 MPa). The thick lines define the boundaries of layers and sub-horizontal tenuous lines give isotherm (°C). A, B, C, D and E mark five locations in the section.

Province suggest that the crust in the study area can be divided into lower, middle and upper crusts, respectively corresponding to mafic granulites (T = 800—900℃ and P = (7.4—10.6)$\times 10^8$ Pa, equivalent to depths of 25—35 km), gneisses (T = 630—650℃ and P = (6.0—8.0)$\times 10^8$ Pa, equivalent to depths of 20—25 km) and the Paleozoic sediments[11,30—34]. As shown in fig. 2(a), we assume that the thickness of the crust is 35 km between the late Paleozoic and early Mesozoic (or early Indo-Sinian). The Paleozoic cover consists of the sandstone-slate and carbonate sedimentary rocks, with a thickness of 15 km in the trough area and 5 km on both of its sides (represented by Layer 1 in fig. 2). The folded basement domain consists of the Proterozoic gneiss and slate, and is 10 km thick in the trough and 20 km thick on both of its sides (represented by Layer 2 in fig. 2). The crystallized basement (represented by Layer 3 in fig. 2) is 10 km thick and consists of amphibolite-granulite rocks. The model simulates a crustal section of 1550 km long and 35 km deep, and the section is approximated by a mesh of 155 × 70, each element of which represents an area of 10 km × 0.5 km (5 km^2).

1.3 Initial thermal and mechanical boundary conditions

1.3.1 Thermal conditions. Considering the special rifting settings in southeastern Hunan Province and the P-T data for the xenoliths from the middle/lower crust[33—35], we assume that the surface temperature of the section, $T(0,0)$, is 25℃ and the geothermal gradient in the crust, $\partial T/\partial z$ $(z, 0)$, is 24℃/km ($0< z <35$ km) so that the temperature of the crust-mantle boundary is 850℃ (equivalent to the surface thermal flux of ca. 65 mW/m^2). The geothermal gradient in the lithospheric mantle, $\partial T/\partial z$ $(z, 0)$, is 10℃/km (35 km$< z <$80 km), corresponding to a temperature of 1300℃ at the base of the lithosphere. Since the geothermal state in the lithosphere should be in equilibrium before another thermal-tectonic activation event, the heat conduction equation was first solved for ca. 24 Ma (without stress load and mechanical deformation computation) to reach a thermal equilibrium state where temperatures in the model become constant. This thermal state (fig. 2(a)) was used to carry out further numerical modeling.

1.3.2 Mechanical parameters. Mechanical modeling of deformation also requires the specification of mechanical parameters including material mechanical properties and stress boundary conditions. The material properties adopted in the model include density, bulk modulus, shear modulus, cohesion, tensile strength, friction angle and dilation angle. In addition, the thermal conductivities of different rocks[36,37] were also considered. Details of these parameters are summarized in table 1. Without the load of external stresses, the lateral boundaries of the model were fixed in the horizontal direction and the base of the model was fixed in the vertical direction to prevent materials from gravitational collapse. To simulate horizontal shortening deformation, a constant displacement rate was applied to the lateral boundaries. The initial stresses for the model reflect stresses in the static lithosphere and follow the formula shown as follows[38]:

$$\sigma_{zz} = \int \rho_{(z)} gzdz, \quad \sigma_{xx} = \sigma_{zz} v/(1-v),$$

where σ_{xx} and σ_{zz} are horizontal and vertical stresses in the lithosphere, respectively, $\rho_{(z)}$ is density as a function of depth, g is gravity, z is depth, and v is Poisson ratio which can be calculated from bulk modulus and shear modulus.

Table 1 Material properties used in the thermal and mechanical models

Lithology	Density /kg • m^{-3}	Cohesion ×10^6/Pa	Tensile strength ×10^6/Pa	Shear mod. ×10^{10}/Pa	Bulk mod. ×10^{10}/Pa	Friction angle /(°)	Dilation angle /(°)	Heat capacity J/kg • K	Heat productivity /μW • m^{-3}
Layer 1 Sandstone, carbonate	2400	5.0	1.5	1.04	1.39	10	2	2000	2.0
Layer 2 Slate, gneiss	2700	11.0	2.0	1.40	1.95	15	2	1200	3.6
Layer 3 Amphibolite, granulate	2900	15.0	2.5	3.60	4.30	15	2	700	0.5

Crustal deformation can be reasonably described by the elastic-plastic constitutive law. In general situations, the strength of the ductile lower crust is much less than that of the lithospheric upper mantle[39]. The crust-mantle boundary (the Moho discontinuity) can thus be generally considered a detachment zone. This allows crust to deform but no significantly disturbing the underlying upper mantle[17]. In this paper, therefore, our discussions focus on temperature perturbations in the crust.

2 Modeling result and discussion

Evidence from experimental petrology indicates that whether or not the anatexis of the continental crust can occur depends critically on the maximum temperature experienced by crustal rocks and hydrous mineral-induced dehydration melting reactions (muscovite, biotite and hornblende)[40,41].

At pressure greater than 3.5×10^8 Pa, the temperature for muscovite- and biotite-induced dehydration melting follows the following empirical relationships[17,42],

$$T_{(Mu)} = 651+9(P/10^8-3.5), \quad T_{(Bi)} = 853+(P/10^8-3.5),$$

where P is pressure in Pa, $T_{(Mu)}$ and $T_{(Bi)}$ are the minimum temperatures for muscovite- and biotite-induced dehydration melting, respectively. The temperatures for hornblende-induced dehydration melting are ca. 900℃ at the pressure of 5.0×10^8 Pa and 920℃ at 10×10^8 Pa[17].

The Indo-Sinian granites in South China are characterized by strongly to slightly peraluminous (A/CNK >1.05) and potassium-rich (K_2O > 4.0%) features, and highly enriched Sr-Nd isotopic compositions, similar to those of the gneisses in South China[2,3]. Generally, peraluminous granitoid melts can be generated by: (i) partial melting of aluminous-rich metamorphic rocks, such as muscovite-biotite schists and gneisses[43]; or (ii) fractionation of aluminum-deficient minerals (hornblende or clinopyroxene)[17,44]; or (iii) partial melting of amphibolites in the pres-

ence of abundant H_2O[45]. It is important to note that the fractionation of aluminum-poor magma and partial melting of lower crust rocks, such as plagioclase amphibolite and granulite, usually produce metaluminous, Na- and Sr-rich liquids, instead of peraluminous and potassium-rich melt at 0.1—1.0 GPa[15,34,44,46]. In addition, the anatexis of continental lower crust will produce only 2%—5% (volume percent) of melts even if the lower crust contains a total abundance of 0.4% (weight percent) H_2O[17,34]. This means that it is very difficult to generate a large volume of peraluminous and potassium-rich granitic batholiths through partial melting of lower crust[34,44]. Therefore, the Indo-Sinian granites in Hunan Province is possibly derived from the muscovite- and/or biotite-induced dehydration melting of middle- and lower-grade metamorphic rocks in the middle/upper crust, rather than from the melting of hornblende-bearing rocks.

Recent studies on the Mesozoic mafic rocks and tectonic evolution in South China suggested that multi-episode lithospheric extensional thinning events had occurred in South China in early Mesozoic[10—14,47]. In the southern Hunan Province, the lithospheric extension and the following basaltic underplating might start in early Mesozoic (±224 Ma)[13,14], the effect of which possibly resulted in the reheating of the lower/middle crust and subsequently induced the remelting of crustal rocks. Alternatively, data from the Indo-Sinian thrusting structural styles, paleogeography and the geochemical characteristics of Indo-Sinian granitoids indicate that the Indo-Sinian tectono-magmatism was triggered by tectonic crustal thickening under the intracontinental convergent conditions[9]. Both mechanisms might contribute to the genesis of the Indo-Sinian granitoids. Below are discussions on their relationship with the remelting of upper/middle crustal rocks.

2.1 A model simulating mafic magma underplating

In this model, we assume that a certain amount of basaltic magma (50 km×1 km) with an initial temperature of 1000℃ was underplated into the middle/lower crust at a depth of about 20 km under the initial equilibrium state as illustrated in fig. 2(a). The perturbation of the geotherm as a result of underplating is shown in fig. 2(b).

The modeling results indicate that the heat conduction from the underplating magma can lead to ambient temperature in the country rocks increasing up to 100—300℃[48,49], triggering the muscovite- and biotite-induced dehydration melting to produce peraluminous and potassium-rich granotoids and/or even the anatexis of amphibolite-facies rocks to produce the slightly aluminous and Sr-rich granitoids. The area of the perturbed domain with temperature over 700°C is four times of that of underplating magma (fig. 2(b)). However, as shown in fig. 3, the thermal perturbation from underplating rapidly increased the temperature of the country rocks and this was followed by rapid temperature decrease. The perturbed temperatures of the country rocks reach the highest level within only ca. 1.5 Ma after the underplating event.

A complete thermal equilibrium (stable state) between the underplating magma and country rocks were reached at ca. 12 Ma after basaltic underplating. The time interval of 12 Ma is consis-

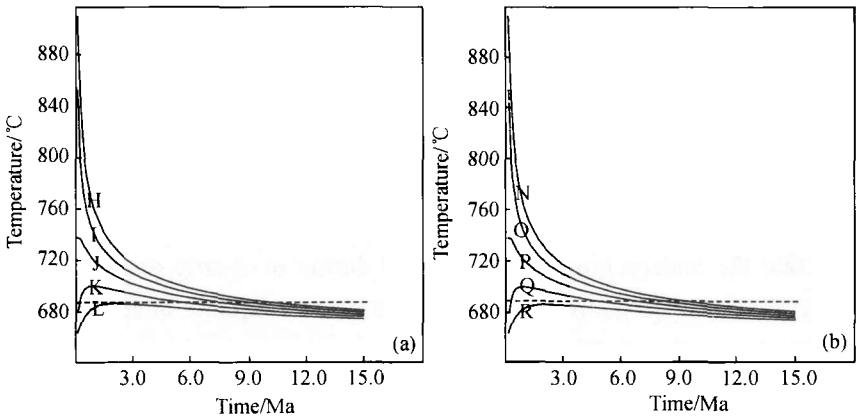

Fig. 3. Modeling results of heat conduction for a scenario where mafic magma with the temperature of 1000℃ is underplated into the lower/middle crust in a stable geothermal state. (a) and (b) illustrate thermal perturbations in the horizontal and vertical directions, away from the underplating magma, respectively. H describes the temperature evolution of a location on the left boundary of the underplating magma (initial temperature = 1000℃). I, J, K and L illustrate temperature variations at 4 locations in country rocks, respectively 10, 20, 30 and 40 km away from the H location (in the horizontal direction). N describes temperature development at a location on the top boundary of the underplating magma (initial temperature = 1000℃). O, P, Q and R represent temperature changes at 4 locations in country rocks, respectively 0.5, 1.0, 1.5 and 2 km away from the N location in the vertical direction. The dashed line is the 690℃ isotherm, above which muscovite-induced dehydration melting occurs.

tent with that of 5—20 Ma reported by other studies[19,50]. These results suggest that crustal anatexis corresponding to the maximum thermal perturbation probably predominantly occurred at ca. 1.5 Ma after the underplating event, that the occurrence of remelting granitoids should be within the time span of 12 Ma after the underplating event, and that the scale of anatexis is strictly limited by the volume of underplating magma. Therefore, it would be very difficult for a small volume of basaltic underplating to provide enough heat energy to generate the Indo-Sinian granitic plutons, which are extensively exposed in Hunan Province, even in South China, unless a large volume of mafic magma had underplated into the middle/lower crust during the period.

If the Indo-Sinian underplating event of the mantle-derived melt were a very important factor contributing to the formation of these contemporary granitoids in Hunan Province, a close spatial and temporal association between the mafic igneous rocks and these intrusions should be observed, unless the lower/middle crust behaved as a very effective "density filter" (i.e. all of the basalt and intermediate magmas were confined to deep levels)[51]. However, the volcanic rocks of lately Indo-Sinian to early Mesozoic ages are sparsely exposed in the southeastern Hunan Province, except for minor gabbro xenoliths with the Sm/Nd isochron age of 224 Ma ($\varepsilon_{Nd}(t)$= +8.8) and ultramafic xenoliths enclosed in late Mesozoic alkaline basalts (130—150 Ma) (fig. 1)[14]. Furthermore, the extensive development of thrusting/stacking structural styles during 260—230 Ma

(muscovite $^{40}Ar/^{39}Ar$ age)[28,52] suggests that the stress field in the study area was dominated by a convergent regime during this period, which is unfavorable to the emplacement of mantle-derived melts into the lower/middle crust. Finally, if the basaltic underplating event had occurred before the tectonically convergent event, then the predominant emplacement ages of these granitoids would have been older than 250 Ma. This is inconsistent with the formation ages of gabbros xenoliths and related mafic volcanic rocks in 224—204 Ma from the southern Hunan Province[13,14], which suggests that the underplating event occurred during or shortly after the tectonic crustal thickening event. Accordingly, the possibility for an extensive basaltic underplating event during Indo-Sinian period is very small. We hence conclude that basaltic underplating is unlikely a predominant mechanism to produce the Indo-Sinian peraluminous granitoids in the region.

2.2 A model simulating tectonic crustal thickening

2.2.1 Tectonic crust thickening, thermal-mechanical perturbation and anatexis. The structural analysis of the Indo-Sinian deformation in the study area shows that a series of NE-trending top-to-NW thrusting/stack structures occurred between the Xuefeng Mountain and the southeastern Hunan Province as a result of the NW-SE oriented compression. We therefore applied a constant shortening displacement rate to the NW side of the model. This is equivalent to subjecting the model (initially in a stable state) to a NW-SE compressional stress field during the period of tectonic crustal thickening.

The modeling results (fig. 2(c)) show that the continental crust is progressively thickened in response to the continuous loading (shortening). As a result of crustal thickening, temperature was significantly perturbed (increased) in the trough region but only slightly modified in the areas on its both sides. When the crust with an initial thickness of 35 km was tectonically thickened to 39 km, or the thickening factor (the crustal thickness after deformation versus the initial thickness) is greater than 1.1, the temperature at the boundary between middle/lower-crust underneath the trough can reach and exceed 700℃. This means that muscovite-induced dehydration melting will occur once the thickening factor is greater than 1.1. However, whether or not the granitic melt from the melting sources can effectively migrate to the crustal-level and form magma chambers is determined by the rheologically critical melt percentage, which is 20%—35% for felsic melts[40,53,54]. As numerical convergent deformation continues in the model, the crust becomes further thickened and the temperature at the boundary between middle/lower crust underneath the trough continues to increase. If the crust thickness is less than 45 km or the thickening factor is less than 1.3, the thermal perturbations from such a tectonic crustal thickening can lead to the melting product of 10%—20% (volume percent) as a result of dehydration melting of gneiss (and/or slate) (refer to fig. 7 published by Clemens et al., 1987[40]). The melt produced at this stage is still not enough to migrate effectively to form a magma chamber due to a lower melting percentage. However, when the continental crust is thickened to > 45 km or the thickening factor is

greater than 1.3, the perturbed temperatures at the boundary between middle/lower crust are about 750℃ and the resultant melt percentage is >20% (volume percent)[40]. The dehydration melting occurred at depths of 18—22 km with a melting thickness of ca. 4 km (fig. 4(a)). This melting percentage is essential for the melt to fractionate and to form granitoid batholiths. In contrast to the trough area, the perturbed temperatures in the areas on both sides of the trough at the boundary between middle and lower crusts are still less than 690℃ (fig. 2(c)), though some temperature increases are observed. These areas correspond to the Yangtze Block and Cathaysian Block.

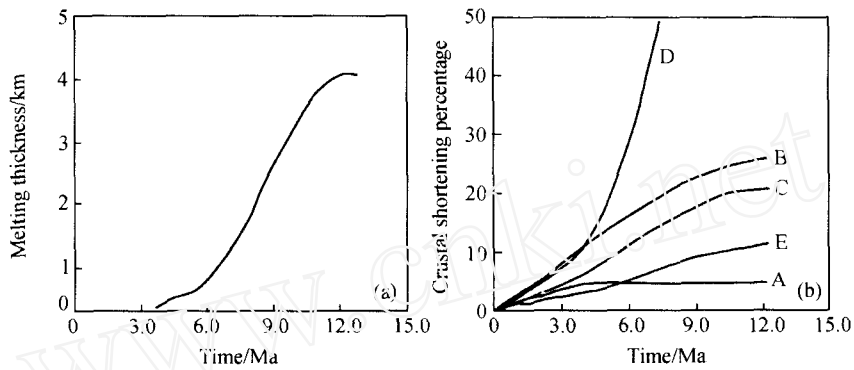

Fig. 4. (a) Melting thickness of muscovite-induced dehydration melting during increasing tectonic crustal thickening. (b) Crust shortening during tectonic thickening in different tectonic situations. See fig. 2(c) for the locations of markers A, B, C, D and E.

In summary, the perturbed temperatures near the boundary between the middle and lower crusts (or between slate/gneiss and amphibolite/granulite) during tectonic crustal thickening can result in muscovite-induced dehydration melting, whereas hornblende- and biotite-induced dehydration melting in the trough is hardly possible unless initial temperatures reach 920°C at the crust-mantle boundary or the metamorphic rocks in middle/lower crust have an extremely high radioactive heat production. The dehydration melting of metamorphic rocks containing hydrous minerals would not take place in the regions on both sides of the trough due to low perturbed temperatures.

2.2.2 Evidence from structural deformation. In our models, heterogeneous crustal deformation occurred while the muscovite-induced dehydration melting took place to generate the Indo-Sinian peraluminous granites in the trough. Fig. 2(c) also shows a significant difference in strain distributions in the upper-middle crust (with depth < 15 km) between the trough and its both sides in the study area. As illustrated in fig. 2(c), deformation was intensively localized along the boundaries of the trough, and the eastern boundary of the trough was more severely deformed than the western boundary. Overall, the trough area displays much greater shear strains than the areas on its both sides (shown with the closed line in fig. 2(c)). Fig. 4(b) illustrates the development of crustal shortening in different tectonic situations, marked as A, B, C, D and E, respectively, where

A represents the eastern Yangtze Block, B denotes the area in western Hunan Province, C for the Lianyuan-Shaoyang area in central Hunan Province, D for the area in southeastern Hunan Province and E for the western Cathaysian Block. When the crust was tectonically thickened up to 45 km, crust shortenings on the eastern and western sides of the trough are 10%—13% and 2%—8%, respectively (A and E in figs. 2(c) and 4(b)). In contrast, the shortenings within the trough are much greater, 45%—220% at the eastern boundary (D in fig. 4(b)), 11%—21% at the central location (C in figs. 2(c) and 4(b)) and 12%—51% at the western boundary (B in figs. 2(c) and 4(b)). It is important to note that these different shortening percentages in different tectonic zones are consistent with the surface structural and deformation styles observed in the study area. For instance, the Jura-type folds are well developed in the eastern Yangtze Block, whereas the southeastern Hunan Province is characterized by compound thrust-folds, thrust-faults and stacking, which represent a much stronger deformation. Thrust-faults dominantly developed in the Xuefeng Mountain in western Hunan Province and this also indicates a weaker deformation situation in comparison with the southeastern Hunan Province. Box folds dominantly developed in the Lianyuan-Shaoyang area in the central Hunan Province[2,3,28,29], representing the weakest deformation in the trough. The modeling results also suggest that the occurrence of the Indo-Sinian peraluminous and potassium-rich granites is coincident with the deformation age in the Hunan-Jiangxi-Guangxi structural zone. Therefore, convergent deformation and tectonic crustal thickening represent an effective mechanism for the development of structural styles and the formation of the Indo-Sinian granites in Hunan Province.

The Mesozoic granites with the crystallization depths of 5—10 km are extensively exposed in South China. This suggests that the upper crust of 5—10 km be denudated since the early Mesozoic in this area. The current crust thickness defined by geophysical profiles is 35—42 km in the Hunan-Jiangxi-Guangxi zone[28,30,31]. Therefore, it can be inferred that the crust has been tectonically thickened to > 42 km during the Indo-Sinian period in the region. In our models, when the continental crust was tectonically thickened up to 43 km, the SE-dipping geometrical interface between the middle/lower crust with low angle can be observed at the depth of 32 km (fig. 2(c)), corresponding to the location of the low-velocity zone in the current crust depth range of 20—25 km in Hunan and Jiangxi provinces[30,31]. It is therefore reasonable to conclude that tectonic crustal thickening is the most likely mechanism to account for the Indo-Sinian tectono-magmatism in Hunan Province.

Thermal-stress readjustment usually takes place within the time span of 10—20 Ma after the ending of tectonic crustal thickening[17]. During stress relaxation in response to the ending of a compression event, small volumes of the basic magma can be possibly underplated near the base of the trough. The involvement of underplating magma, as if acting as a catalyst, will induce the dehydration melting of gneisses to increase melt percentage (possibly larger than ca. 50% (volume percent)) which will greatly facilitate melt migration[40]. The $^{40}Ar/^{39}Ar$ age of muscovite for the

mylonites from the thrusting zone in the Hunan-Jiangxi-Guangxi zone[28,52] suggested that the tectonic thickening event occurred at the time interval of 260—230 Ma. But the gabbro xenoliths in Daoxian County suggested that the earliest basic magma underplating might occur at ca. 224 Ma (Sm-Nd isochron age). This time interval nicely corresponds to that of the thermal-stress relaxation after the stacking event. The occurrence of small-scale magma underplating is therefore possible, as indicated by the gabbro xenoliths in Daoxian County during the thermal-stress relaxation after the ending of the tectonically thickening event.

3 Conclusion

The thermal-mechanical relationships between the genesis of the Indo-Sinian peraluminous and potassium-rich granitoids and either the contemporary basic magma underplating or the tectonic thickening of the continental crust have been numerically simulated in this paper. The underplating of a small volume of basic magma into the middle/lower crust will trigger the dehydration melting of hydrous minerals-bearing metamorphic rocks to generate the peraluminous and potassium-rich liquids. The location of magma underplating at the middle/lower crust levels should correspond to the central locations of the granitic melt generated, but the thermal perturbation effects of this mechanism are limited in terms of time span and spatial extent. Tectonic crustal thickening can lead to a significant increase in temperature at the boundary between middle and lower crusts in the trough region. When the thickening factor is up to 1.1, temperature at this boundary can be greater than 690°, which is hot enough to trigger the muscovite-induced dehydration melting to produce the peraluminous and potassium-rich granitic liquid. When the thickening factor is greater than 1.3, the muscovite-induced dehydration melting will produce >20% (volume percent) melt in the trough region, which can effectively migrate into magma chambers at shallower crustal levels to form the granitic batholiths. However, the perturbed temperature in the crust on both sides of the trough is not high enough to induce the dehydration melting of any kind of hydrous mineral-bearing metamorphic rocks. In combination with the geological data from deformation styles in the region and rare outcrops of the Indo-Sinian volcanic rocks, it is reasonable to conclude that the generation of Indo-Sinian peraluminous and potassium-rich granitoids is predominantly attributed to the tectonic crustal thickening/stacking rather than basaltic underplating.

Acknowledgements The authors are grateful to the anonymous reviewers. Their constructive reviews helped to improve the manuscript. This work was supported by the Chinese Academy of Sciences (Grant Nos. KZCX2-102 and KZCX3-113), the Ministry of Science and Technology of China (Grant No. G1999043209) and the National Natural Science Foundation of China (Grant No. 40002007).

References

1. Hunan Bureau of Geology and Resources, Hunan Regional Geology (in Chinese), Beijing: Geological Press, 1988.
2. Zhuang Jinliang, Liu Zhongwei, Tan Bixiang et al., The relationship between dioritic intrusions and mineralization in southern Hunan and the prognosis of concealed ore-deposits, Hunan Geology (in Chinese), 1988, 4(Supp): 31—72.
3. Tong Qianming, The metallogenic series of the important nonferrous-precious metal deposits and their metallogenic pat-

tern, Hunan Geology (in Chinese), 1997, 9(Supp): 17—33.

4. Hsu, K. J., Li, J. L., Chong, H. H., Tectonic of South China: Key to understanding West Pactific geology, Tectonophys., 1990, 183: 9—39.
5. Chen Haihong, Multi-island-ocean collisional orogen: An example of Indo-Sinian orogenic belt in South China, Frontier of Earth Sciences, 1998, 5: 95—102.
6. Rowley, D. B., Ziegler, A. M., Nie, G., Comment on "Mesozoic overthrust tectonics in South China", Geology, 1997, 17: 384—386
7. Chen Xu, Xu Jiayu, Rowley, D. B. et al., Is the early Paleozoic Banxi ocean in South China necessary? Geological Review (in Chinese), 1995, 5: 389—398.
8. Gilder, S. A., Gill, J., Coe, R. S. et al., Isotopic and paleomagnetic constraints on the Mesozoic tectonic evolution of South China, Journal of Geophysical Research, 1996, 107(B7): 16137—16154.
9. Jin Wenshan, Sun Dazhong (eds), The continental Deep-Crust Structure in South China and Its Evolution (in Chinese), Beijing: Geologic Press, 1997.
10. Wang Yuejun, Fan Weiming, Guo Feng et al., Petrological and geochemical characteristics of Mesozoic granodioritic intrusions in Southeast Hunan Province, South China, Acta Petrologica Sinica (in Chinese), 2001, 17(1): 169—175.
11. Wang Yuejun, Fan Weiming, Guo Feng et al., U-Pb dating of early Mesozoic granodioritic intrusions in southeastern Hunan Province, South China and its petrogenetic implication, Science in China, Ser. D, 2002, 45(3): 280—288.
12. Liu Yimao, Dai Tongmo, Lu Huanzhang et al., $^{40}Ar/^{39}Ar$ and Sm/Nd isotopic ages of the lithogenesis and mineralization of the Qianlishan granite? Science in China (in Chinese), Ser. D, 1997, 27(5): 425—430.
13. Zhao Zhenghua, Bao Zhiwei, Zhang Boyou, Geochemistry of Mesozoic basaltic rocks in southern Hunan Province, Science in China, Ser. D, 1998, 41(Supp.): 102—112.
14. Guo Feng, Fan Weiming, Lin Ge et al., Sm-Nd dating and petrogenesis of Mesozoic gabbro xenolith in Daoxian County, Hunan Province, Chinese Science Bulletin, 1997, 42(17): 1814—1816.
15. Gaudemer, Y., Jaupart, C., Tapponnier, P., Thermal control on the post-orogenic extension in collision belts, Earth & Planet. Sci. Lett., 1988, 89: 48—62.
16. de Yereo, J. J., Lux, D. R., Guidotti, C. V., The role of crustal anatexis and magma migration in the thermal evolution of regions of thickened continental crust in evolution of metamorphic belts, in Evolution of Metamorphic Belts (ed. Daly, J. S.), London: Mem. Geol. Soc. Lond., 1989, 187—202.
17. Patiño-Dounce, A. E., Humphreys, E. D, Johnston, A. D., Anatexis and metamorphism in tectonically thickened continental crust examplified by the Sevier hinterland, western North America, Earth and Planet. Sci. Lett., 1990, 97: 290—315.
18. Liu, M., Intrusion and underplating of mafic magma: Thermal-rheological effect and implications for Tertiary tectonomagmatism in the North American Cordillera, Tectonophysics, 1994, 237(3): 175—187.
19. Koyaguchi, T., Kaneko, K., A two-stage thermal evolution model of magmas in continental crust, J. Petrol., 1999, 40(2): 241—254.
20. Ranalli, G., Rheology of the Earth, London: Allen & Unwin, 1987, 1—366.
21. Vermeer, P. A., de Borst, R., Non-associated plasticity for soils, concrete and rock, Heron, 1984, 29: 1—64.
22. Hobbs, B. E., Muhlhaus, H. B., Ord, A., Instability, softening and localization of deformation, in Deformation Mechanisms, Rheology and Tectonics (eds. Knippe, R. J., Rutter, E. H.), London: Geol. Soc. Spec. Pub., 1990, 54: 143—165.
23. Ord, A., Deformation of rock: A pressure-sensitive, dilatants material, PAGEOPH, 1991, 137: 337—366.
24. Edmond, J. M., Paterson, M. S., Volume changes during the deformation of rocks at high pressures, Int. J. Rock Mech. & Mining Sci., 1972, 9: 161—182.
25. Li, Z. X., Li, X. H., Kinny, P. D. et al., The breakup of Rodinia: Did it start with a mantle plume beneath South China?

Earth and Planetary Science Letters, 1999, 173: 171—181.

26. Mu Chuanglong, Qiu Dongzhou, Wang Liquan et al., Permian Succession Paleogeography in Hunan-Hubei- Jiangxi Provinces and Oil Gas (in Chinese), Beijing: Geological Press, 2000, 1—148
27. Wang Liting, Permian Lithofacies-Paleogeography and Mineralization (in Chinese), Beijing: Geological Press, 1994.
28. Chen, A., Mirror-image thrusting in the South China orogenic belt: Tectonic evidence from western Fujian, southeastern China, Tectonophysics, 1999, 305: 497—519.
29. Chen Haihong, The structural constraints of foreland basin: An example from the Mesozoic Yuanma basin in western Hunan Province, in Sea-continental lithospheric structure and evolution in southeastern China (ed. Li Jiliang) (in Chinese), Beijing: Chinese Science and Technology Press, 1992, 17—31.
30. Yuan, X. C., Zuo, Y. M., Cai, Y. L. et al., The structure of the lithosphere and the geophysics in South China Block, in Progress in Geophysics in China in the 1980s (ed. the editorial board of Bulletin of Geophysic) (in Chinese), Beijing: Science Press, 1989, 243—249.
31. Qin Baohu, The deep-structure in Hunan Province revealed from Taiwan-Heishui geological section, Hunan Geology (in Chinese), 1991, 10(2): 89—96.
32. Lin Ge, Fan Weiming, Guo Feng et al., The crust-mantle transitional zone and its tectonic evolution, Geotectonic et Metallogenia (in Chinese), 1998, (Supp): 11—18.
33. Guo Feng, Fan Weiming, Lin Ge et al., Petrology and geochronology of gnesiss xenolith in Daoxian County, Hunan Province, J. Changchun Institute of Geology (in Chinese), 1997, 27(1): 25—30.
34. Zhong Yingxian, Liu Yuanchao, The preliminary research of the Fuziyan intrusion and its granulite xenoliths in Daoxian County, Hunan Province, J. Chengdu Institute of Geology (in Chinese), 1993, 20(1): 56—61.
35. Carter, N. L., Anderson, D. A., Creep and creep rupture of granitic rocks, Washington: Am. Geophys. Union. Geophys. Monogr., 1982, 24: 61—82.
36. Wollenberg, H. A., Smith, A. P., Radiogenic heat production of crustal rocks: A compilation from unpublished data and the geochemical literature, Trans. Am. Geophys. Union, 1984, 65: 1—1121.
37. Zhang, Y., Scheibner, E., Hobbs, B E., Lithospheric structure in southeast Australia: A model based on gravity, geoid and mechanical analyses, in: Structure and Dynamics of the Australian Lithosphere (eds. Braun, J., Dooley, J., Goleby, B.), Geodynamics Series 26, Washington: Amer. Geophysic. Union, 1998, 89—108.
38. Jaeger, J. C., Cook, N. G. W., Fundamentals of Rock Mechanics, London: Chapman and Hall, 1979, 1—593.
39. Kusznir, N. J., Park, R. G., The extensional strength of the continental lithosphere: Its dependence to geothermal gradient, and crustal composition and thickness, in: Continental Extensional Tectonics (eds. Coward, M. C., Dewey, J. F., Hancock, P. L.), London: Geol. Soc. Spec. Publ., 1987, 28: 35—52.
40. Clemens, J. D., Vielzeuf, D., Constraints on melting and magma production in the crust, Earth and Planetary Science Letters, 1987, 86: 287—306.
41. Gardien, V., Thompson, A. B., Grujic, D. et al., Experimental melting of biotite+plagioclase+quartz±muscovite assemblages and implications for crusting melting, J. Geophys. Res., 1995, 100: 15581—15591.
42. Tompson, A. B., Fertility of crustal rocks during anatexis, Earth Sci., 1996, 87: 1—10.
43. Miller, C. F., Are strongly peraluminous magmas derived from pelitic sedimentary sources? J. Geol., 1995, 93: 673—689.
44. Zen, E., Aluminum enrichment in silicate melts by fractional crystallization: Some mineralogic and petrographic constrains, J. Petrol., 1986, 27: 1095—1117.
45. Ellis, D. J., Thompson, A. B., Subsolidus and partial melting reactions in the quartz-excess $CaO+MgO+Al_2O_3+SiO_2+H_2O$ system under water-excess and water-deficient conditions to 10 kbar: Some implications for the origin of peraluminous melts from mafic rocks, J. Petrol., 1986, 27: 91—121.

46. Rutter, M. J., Wyllie, P. J., Melting of vapour-absent tonalite at 10 kb to simulate dehydration-melting in the deep crust, Nature, 1988, 331: 159—160.
47. Li, X. H., Cretaceous magmatism and lithospheric extension in Southeast China, Journal of Asian Earth Sciences, 2000, 18: 293—305.
48. Bergantz, W. V., Underplating and partial melting: Implications for melt generation and extraction, Science, 1989, 245: 1093—1095.
49. Fountain, D. M., Growth and modification of lower continental crust in extended terrians: The role of extension and magmatic underplating, in Properties and Processes in Earth's Lower Crust (eds. Mereu, R. F., Muller, S., Fountain, M. F.), Washington: Am. Geophys. Union, Geophys. Monogr. Ser., 1989, 51: 287—299.
50. Spear, F. S., Peacock, S. M., Program and manual and computer exercises for the calculation of metamorphic phase equilibria, pressure-temperature-time paths and thermal evolution of orogenic belts (Report), New York: Rensselaer Polytech. Inst. Troy, 1990.
51. Jung, S., Hoernes, S., Mezger, K., Geochronology and petrogenesis of Pan-African, syn-tectonic S-type and post-tectonic A-type granite (Namibia): Products of melting of crustal sources, fractional crystallization and wall rock entrainment, Lithos., 2000, 50: 259—287.
52. Peng Shaomei, Fu Lifen, Zhou Guoqiang, Tectonic Evolution of Yunkai Block and the Shearing Anatexis of the Gneissic Granites (in Chinese), Wuhan: China University of Geosciences Press, 1995, 1—165.
53. Arzi, A. A., Critical phenomena in the rheology of partially melted rocks, Tectonophysics, 1978, 44: 173—184.
54. Brown, M., The generation, segregation, ascent and emplacement of granite magma with the migmatite-to-crustally-derived granite connection in thickened orogens, Earth Sci. Reviews, 1994, 36: 83—130